Pergamon

Bioorganic & Medicinal Chemistry 10 (2002) 2015–2022

BIOORGANIC & MEDICINAL CHEMISTRY

Insight into the Stereochemistry in the Inhibition of Carboxypeptidase A with *N*-(hydroxyaminocarbonyl)phenylalanine: Binding Modes of an Enantiomeric Pair of the Inhibitor to Carboxypeptidase A

Jae Hyun Cho,[a] Dong H. Kim,[b,*] Sang J. Chung,[b] Nam-Chul Ha,[c] Byung-Ha Oh[c] and Kwan Yong Choi[a]

[a]*National Research Laboratory for Protein Engineering, Pohang University of Science and Technology, San 31Hyoja-dong, Pohang 790-784, Republic of Korea*

[b]*Center for Biofunctional Molecules, Pohang University of Science and Technology, San 31Hyoja-dong, Pohang 790-784, Republic of Korea*

[c]*National Creative Research Initiative Center for Biomolecular Recognition, Pohang University of Science and Technology, San 31Hyoja-dong, Pohang 790-784, Republic of Korea*

This paper is dedicated to Professor Sang Chul Shim on the occasion of his retirement.

Received 13 August 2001; accepted 4 December 2001

Abstract—Both D- and L-isomers of *N*-(hydroxyaminocarbonyl)phenylalanine (**1**) were shown to have strong binding affinity towards carboxypeptidase A (CPA) with D-**1** being more potent than its enantiomer by 3-fold (Chung, S. J.; Kim, D. H. *Bioorg. Med. Chem.* **2001**, *9*, 185.). In order to understand the reversed stereochemical preference shown in the CPA inhibition, we have solved the crystal structures of CPA complexed with each enantiometer of **1** up to 1.75 Å resolution. Inhibitor L-**1** whose stereochemistry belongs to the stereochemical series of substrate binds CPA like substrate does with its carbonyl oxygen coordinating to the active site zinc ion. Its hydroxyl is engaged in hydrogen bonding with the carboxylate of Glu-270. On the other hand, in binding of D-**1** to CPA, its terminal hydroxyl group is involved in interactions with the active site zinc ion and the carboxylate of Glu-270. In both CPA·**1** complexes, the phenyl ring in **1** is fitted in the substrate recognition pocket at the S_1' subsite, and the carboxylate of the inhibitors forms bifurcated hydrogen bonds with the guanidinium moiety of Arg-145 and a hydrogen bond with the guanidinium of Arg-127. In the complex of CPA·D-**1**, the carboxylate of the inhibitor is engaged in hydrogen bonding with the phenolic hydroxyl of the down-positioned Tyr-248. While the L-**1** binding induces a concerted movement of the backbone amino acid residues at the active site, only the downward movement of Tyr-248 was noted when D-**1** binds to CPA. © 2002 Elsevier Science Ltd. All rights reserved.

Introduction

Carboxypeptidase A (CPA) is one of the most extensively studied zinc containing proteolytic enzymes and serves as a prototypical enzyme for a large family of metalloproteases that play important roles in numerous physiological and pathological conditions.[1,2] The enzyme removes preferentially the C-terminal amino acid residue having an aromatic or hydrophobic aliphatic side chain from peptide substrates. The catalytically essential zinc ion that is present at the active site of the enzyme is coordinated to His-69, Glu-72, and His-196. A water molecule is bound to the metal ion loosely as the fourth ligand. The other important residues at the active site of CPA are Glu-270, Arg-145, and Arg-127. It has been proposed that the carboxylate of Glu-270 abstracts a proton from the zinc bound water molecule, generating a hydroxide ion that attacks on the scissile peptide bond of the enzyme-bound substrate to generate a tetrahedral transition state.[2] The guanidinium moiety of Arg-145 is suggested to form hydrogen bonds to the C-terminal carboxylate of substrate, and Arg-127 activates the scissile peptide bond of the enzyme-bound

*Corresponding author. Tel.: +82-54-279-2101; fax: +82-54-279-5877; e-mail: dhkim@postech.ac.kr

0968-0896/02/$ - see front matter © 2002 Elsevier Science Ltd. All rights reserved.
PII: S0968-0896(01)00429-1

substrate through hydrogen bonding and stabilizes the tetrahedral transition state that is generated in the catalytic hydrolysis reaction.[3] In addition, the active site contains a hydrophobic pocket, the primary function of which is to recognize substrate by accommodating the aromatic or hydrophobic aliphatic side chain in the P_1' residue of substrate.[1,2] CPA has been used as a model enzyme for developing design strategy of inhibitors that are effective for zinc proteases of medicinal interest.[4–7] Most CPA inhibitors are designed by incorporating a zinc ligating functionality into P_1' substrate molecule. Widely used zinc-ligating groups for the design of zinc proteases inhibitors include carboxylate, sulfhydryl, phosphate, phosphonamide, and hydroxamate, of which the hydroxamate has been most frequently utilized because of its high propensity to form a thermodynamically stable chelate complex with a zinc ion.[8]

Recently, we have reported that *N*-(hydroxyaminocarbonyl)phenylalanine (**1**) is a potent inhibitor for CPA,[9] which was designed exploiting the metal chelating property reported for hydroxyurea.[10] In the evaluation of the inhibition potency of each enantiomer of **1**, we have found to our surprise that the inhibitor having the D-configuration (D-**1**), that is, the stereochemistry of unnatural amino acids is more potent than L-**1** by about 3-fold.[9] However, in the case of aminocarbonylphenylalanine (**2**) in which the terminal hydroxyl in **1** is deprived, only the L-form showed inhibitory activity albeit weak (Table 1).[9] The interesting stereochemical behavior shown by these inhibitors prompted us to undertake a X-ray structural investigation on the CPA complexes formed with the inhibitors. We report herein the results of the study, which sheds light on the origin of the reversed stereochemical preference in the inhibition of CPA by the hydroxyurea-type inhibitors.

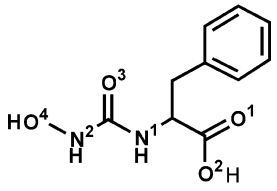

1

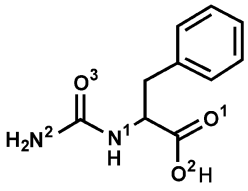

2

Table 1. Inhibitory constants for CPA inhibition

Inhibitor	K_i (μM)[a]
L-1	4.6±0.38
D-1	1.5±0.10
L-2	19±1.1
D-2	—

[a]Ref 9.

Results

The crystal structures of CPA complexed with each of L-**1**, D-**1** and L-**2** were solved by molecular replacement using the crystal structure of uninhibited CPA.[15] The active site zinc ion was omitted until the final refinement of the enzyme structure is obtained. Figure 1 shows the streroview of the difference electron density at the active site region of inhibitor-bound CPA. The electron density maps clearly show that one molecule of each inhibitor is bound to the enzyme. Distances of important interactions between CPA and the inhibitors in the complexes are listed in Table 3.

Inhibitor L-**1** that belongs to the same stereochemical series as the P_1' substrate residue appears to bind CPA in a fashion analogous to the binding of substrate (Fig. 2a). The carboxylate of L-**1** is engaged in hydrogen bonding with both nitrogen atoms in the guanidinium moiety of Arg-145 and one of nitrogen atoms of the guanidinium of Arg-127. The benzene ring of the inhibitor is accommodated in the S_1' hydrophobic pocket, the primary substrate recognition site of CPA. These binding interactions are reminiscent of those reported for the CPA complex with Gly-L-Tyr,[16] and are found in the complexes of CPA•D-**1** and CPA•L-**2** as well. The aromatic side chain of Tyr-248 is found in the 'so called' down position, but its phenolic hydroxyl is not engaged in hydrogen bonding with the carboxylate of the inhibitor. Instead, it forms a hydrogen bond with a water molecule that rests at a position separated from the carboxylate of the inhibitor by 2.88 Å. Thus, the phenolic hydroxyl interacts indirectly with the carboxylate of the inhibitor. This type of binding mode has not been reported previously in CPA•inhibitor complexes. In most of ligand-bound CPAs, the phenolic hydroxyl of the down positioned Tyr-248 is involved in a direct hydrogen bond with the terminal carboxylate of the ligand.[2,16] For example, the phenolic oxygen atom of the down positioned Tyr-248 was shown to be separated by 2.8 Å from one of the terminal carboxylate oxygens of CPA-bound Gly-L-Tyr, a slowly hydrolyzing substrate of CPA.[16] There was observed a water molecule which is hydrogen bonded to a carboxylate oxygen of Glu-270 (Fig. 2a). The zinc-bound water molecule that is found in the native CPA is absent in this complex. The carbonyl oxygen of the inhibitor is separated from the active site zinc ion by 2.06 Å, suggesting that it is ligated to the zinc ion. The terminal hydroxyl group of the inhibitor is engaged in hydrogen bonding with each of carboxylate oxygen atoms of Glu-270 with bonding distances of 2.84 and 2.91 Å. In addition, a hydrogen bond is formed between N^1 of L-**1** and one of the carboxlyte oxygen atoms of Glu-270. We were surprised by the binding mode because we had expected that the terminal hydroxyaminocarbonyl in L-**1** would chelate the active site zinc ion just like the hydroxamate of hydroxamate-bearing CPA inhibitors chelates the zinc ion in their binding to the enzyme.[17–20] Figure 2c depicts the binding mode of L-**2**, which is essentially identical to that of L-**1** except that the hydrogen bond between the terminal hydroxyl of L-**1** and the carboxylate of Glu-270 is absent. We note, however, that the N^2 of L-**2** is separated by 3.18 Å from one of carboxylate oxygen atoms of Glu-270, suggesting that a weak hydrogen bond is formed between them. This weak hydrogen bond appears to partially compensate the loss of the binding energy resulted by the absence of the terminal hydroxyl group in L-**1**. The small reduction (0.84 kcal mol^{-1}) of binding energy that is caused by the removal of the hydroxyl group in L-1 may thus be rationalized.

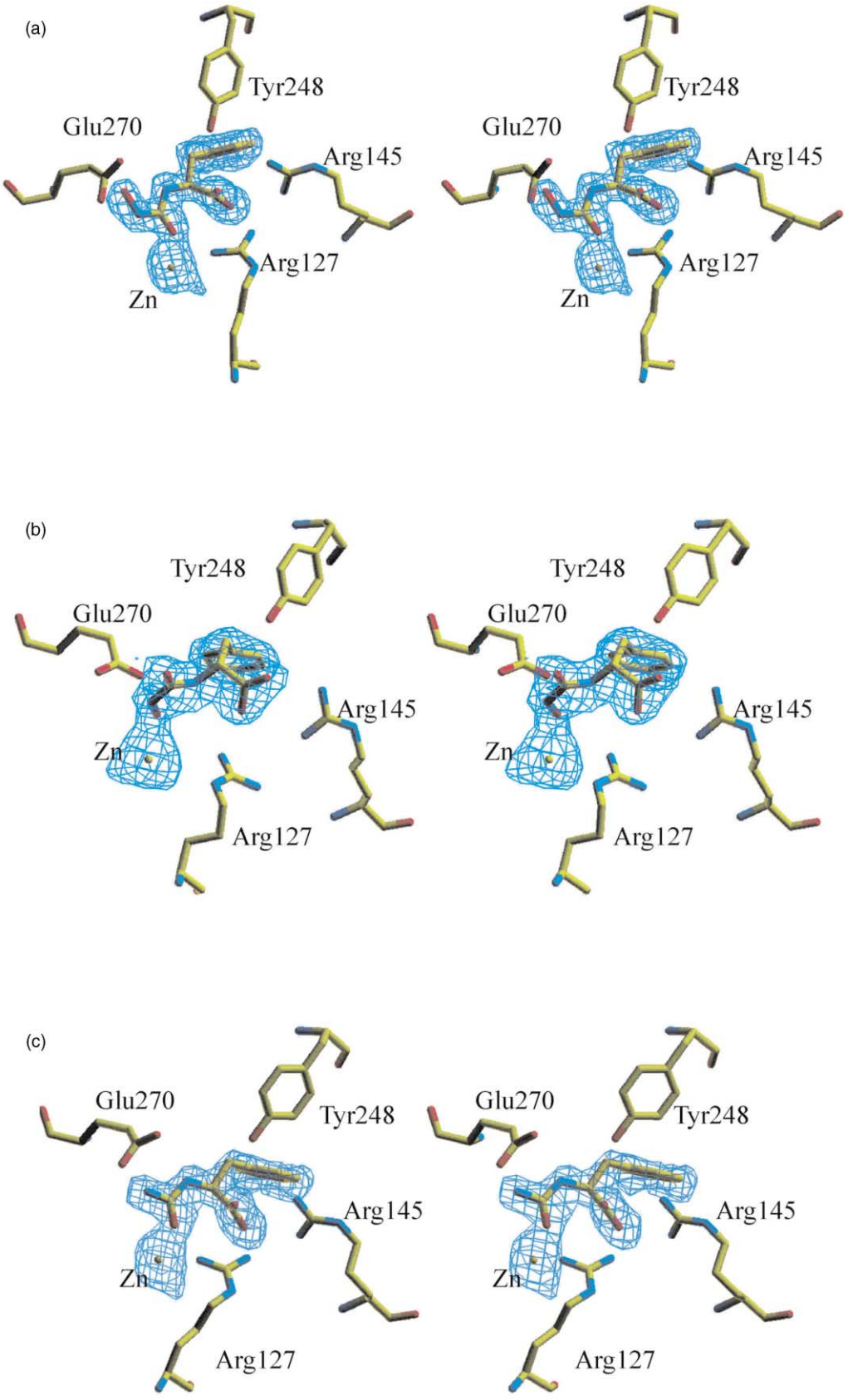

Figure 1. Difference electron density maps for (a), CPA•L-**1,** (b) CPA•D-**1,** and (c) CPA•L-**2** complexes generated with Fourier coefficient $|F_O| - |F_C|$ and phases calculated from the final model omitting the bound inhibitors.

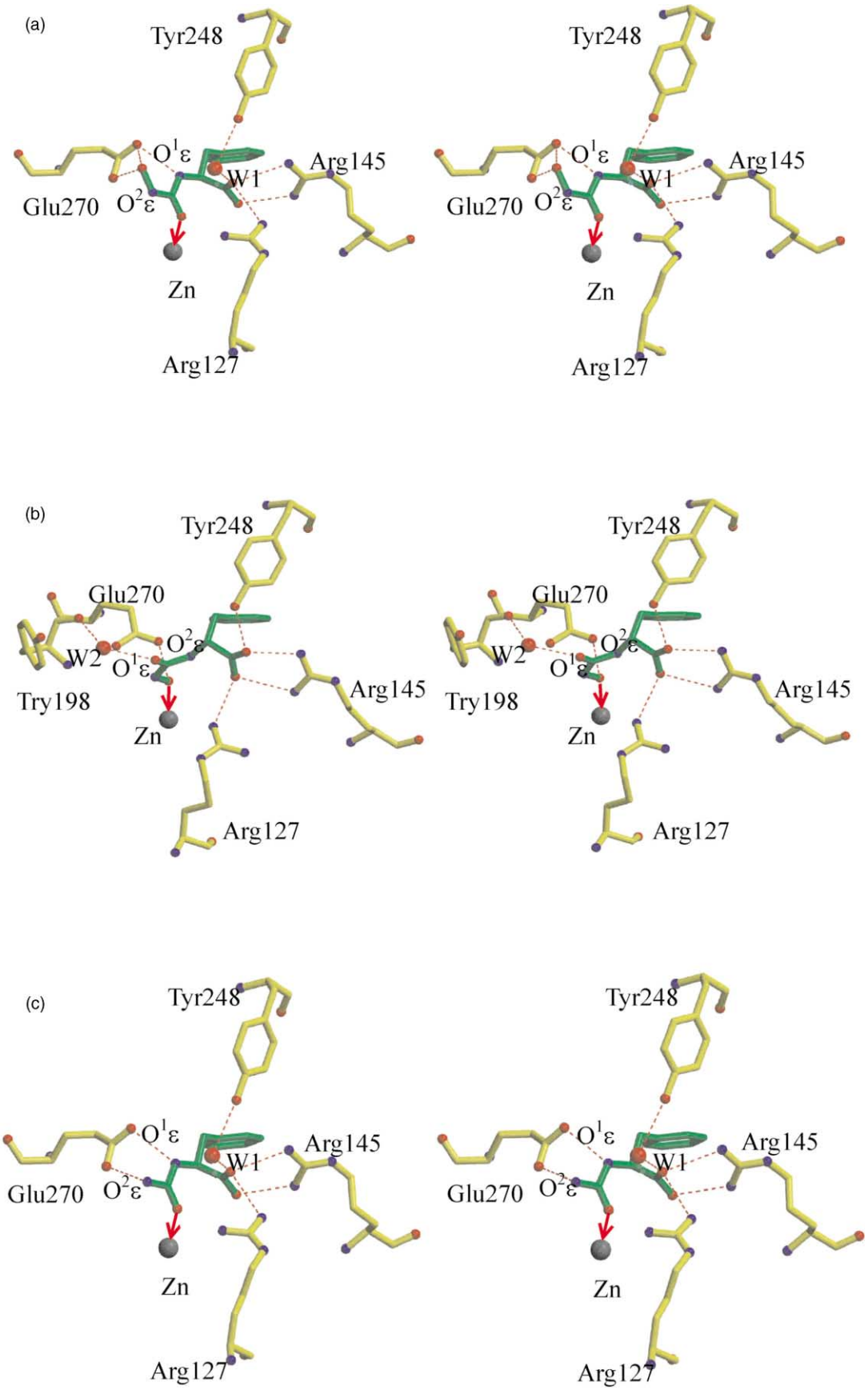

Figure 2. Relaxed stereoview of CPA inhibitor complexes: (a) CPA·L-**1,** (b) CPA·D-**1** and (c) CPA·L-**2**..

The binding mode of D-**1** to the zinc ion is found to be very different from that of L-**1** and L-**2**, although the carboxylate and the phenyl ring of D-**1** bind CPA in a fashion analogous to that exhibited by L-**1** (Fig. 2b). The active site zinc ion is ligated by the terminal hydroxyl oxygen of D-**1**: the terminal hydroxyl oxygen atom is 2.17 Å apart from the active site zinc ion, which is well within the distance to form a coordinative bond with the zinc ion. The terminal hydroxyl of D-**1** is also engaged in hydrogen bonding with one of carboxylate oxygens of Glu-270 as shown by the interatomic distance of 2.67 Å (Table 2). It appears therefore that the carboxylate may function as a general base, causing to reduce the pK_a value of the hydroxyl, and, as a result, the binding interactions of the hydroxyl to the zinc ion are intensified. The carbonyl oxygen in D-**1** is positioned away from the zinc ion and is engaged in hydrogen bonding with the water molecule that is hydrogen bonded to the peptide carbonyl of Tyr-198. Another noticeable difference found in the complex of CPA with D-**1** in comparison with the CPA•L-**1** complex is that the phenolic hydroxyl of the down-positioned Tyr-248 is rested within hydrogen bonding proximity (2.94 Å) to the carboxylate of the inhibitor. Such hydrogen bond is commonly observed in CPA·inhibitor complexes.[2,16] A stereoview comparing the structure of CPA·L-**1** with that of CPA· D-1 is shown in Figure 3.

Glu-270, Arg-145, and Arg-127 residues play critical roles in the CPA catalyzed proteolysis reaction. Upon binding of L-**1** to CPA, the side chains of these residues are shown to undergo noticeable movements towards the inhibitor and engage in interactions with functional groups in the inhibitor (Fig. 4a). The guanidinium moiety in Arg-145 moves towards the carboxylate of L-**1** and the guanidinium of Arg-127 undergoes bond rotation to engage in a hydrogen bond formation with the carboxylate oxygen of L-**1**. On the other hand, the carboxylate of Glu-270 is pushed outward by the hydroxyl of L-**1**. It is interesting to note that with the exception of Tyr-248 the amino acid residues that undergo conformational changes upon binding of L-**1** remain essentially unchanged when D-1 forms complex with CPA.

The hydrophobic pocket present at the S_1' subsite of CPA is known to accommodate the aromatic ring in the side chain of the C-terminal amino acid residue of substrate. It can be seen in Figure 3 that the benzene ring of both inhibitors, L-**1** and D-**1** are rested at about the same loci in the pocket, although the rest of the each molecule is positioned quite differently as described above. The catalytically essential zinc-bound water molecule that is found in the native CPA is not seen in all the CPA·inhibitor complexes examined in the present study. In consistent with the observations, X-ray crystallographic studies[16,21–24] and molecular dynamic calculations[25] carried out with the CPA·inhibitor complexes have suggested that the zinc-bound water molecule becomes mobile and is easily displaced upon inhibitor binding to the enzyme.

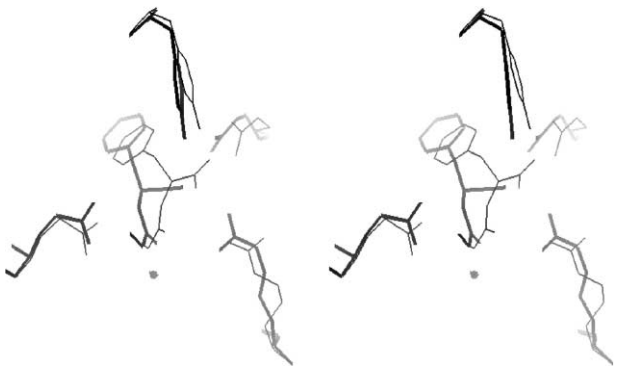

Figure 3. Superimposed stereoview of the active site region of the CPA•inhibitor complexes. Thick line represents CPA•L-**1** complex and thin line shows CPA•D-**1** complex.

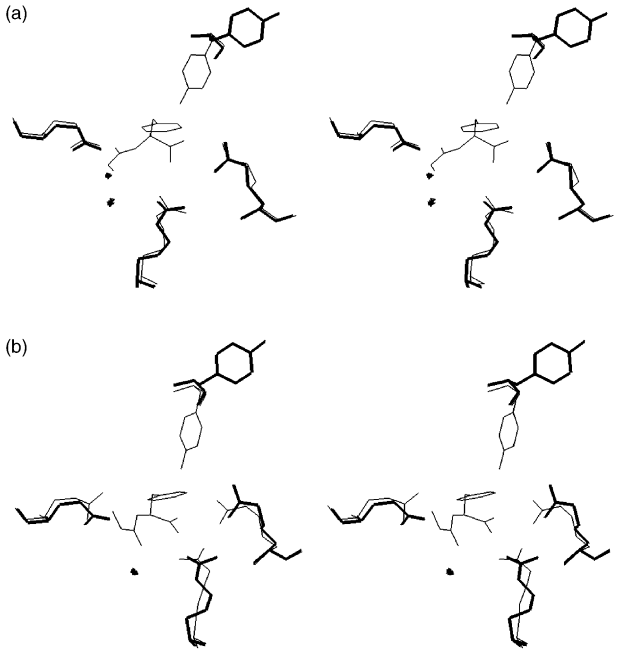

Figure 4. Stereoview of the active site region of the native CPA (thick line) compared with that of (a) CPA•L-**1** and (b) CPA•D-**1**.

Discussion

Both stereoisomers of **1** in a mirror image relationship were reported to have strong binding affinity towards CPA with the D-form being more potent by 3-fold (Table 1).[9] We have investigated this unexpected reversal of stereochemical preference in binding of **1** to CPA by the X-ray crystallographic method. The CPA complex with L-**1** reveals that the inhibitor binds to CPA as substrate does with its carbonyl oxygen coordinating to the active site zinc ion (Fig. 2a).[16] The terminal hydroxyl of the inhibitor is involved in hydrogen bonding with the carboxylate of Glu-270. We were surprised by the finding because we expected that the hydroxyaminocarbonyl moiety of the inhibitor would bind the zinc ion in a bidentate fashion as hydroxamate does. The carboxylate of L-**1** is engaged in hydrogen bonding with the guanidinium moieties of Arg-145 and Arg-127 and the phenyl ring is fitted in the substrate recognition pocket

at the S_1' subsite of CPA. The active site undergoes a considerable conformational change upon binding of L-**1** to CPA (Fig. 4a). The binding mode of L-**2** which lacks the terminal hydroxlyl of L-**1** is essentially the same as that of L-**1**. The hydrogen bond between the Glu-270 carboxylate and the terminal hydroxyl of L-**1** in the CPA•L-**1** complex is absent in the CPA•L-**2** complex, but instead a new weak hydrogen bond is formed in the binding of L-**2** to CPA: the terminal amino nitrogen atom in L-**2** is engaged in weak hydrogen bonding with one of the Glu-270 carboxylate oxygen atoms (Fig. 2c). The carbonyl oxygen of the urea moiety in L-**2** ligates the active site zinc ion.

The binding mode of D-**1** is found to be significantly different from that of L-**1**. Most noticeably, the terminal hydroxyl group of D-**1** is 2.17 Å apart from the active site zinc ion, indicating that in the binding of D-**1** to CPA the hydroxyl oxygen rather than the carbonyl oxygen ligates the metal ion (Fig. 2b). The hydroxyl is also involved in a hydrogen bond with the carboxylate of Glu-270. A hydrogen bond is formed between one of oxygen atoms of the carboxylate of the inhibitor and the phenolic hydroxyl of the down positioned Tyr-248. No such direct binding interaction is found in the complex of CPA•L-**1**, although the Tyr-248 is in the down position. This difference in the binding interactions may be responsible for at least in part the 3-fold stronger complexing affinity shown by D-**1** relative to L-**1**. It is noteworthy that in contrast to L-**1**, D-**1** does not cause significant conformational change of CPA except the downward movement of Tyr-248 when it binds the enzyme (Fig. 4b). The present study reveals that L-**1** which belongs to the same stereochemical series as substrate binds CPA more like substrate does, but D-**1** which bears stereochemistry opposite of substrate binds quite differently from the binding of substrate with its terminal hydroxyl oxygen rather than the carbonyl oxygen ligating the active site zinc.

In many cases, the biological activity of a racemic drug rests only on one enantiomer. For example, methyldopa owes its antihypertensive effect exclusively to the (*S*)-isomer.[26] However, our understanding on the stereoselective biological effect is very superficial and we can hardly predict which enantiomer is responsible for the observed biological activity. The present study provides some insight into how a pair of enantiomeric inhibitors may be accommodated by a common binding site with dissimilar binding affinity.

Experimental

Crystallization. Bovine carboxypeptidase A was purchased from Sigma. The inhibitors were prepared as described previously.[9] To remove toluene present in the protein sample, the stock solution of CPA was purified using desalting column (Pharmacia) and then diluted to 10 mg mL^{-1} with 0.02 M Tris–HCl (pH 7.5) containing 1.2 M LiCl. An aliquot of 5 μL of the solution on a microdialysis button (Hampton research) was dialyzed in a low salt buffer containing 0.14 M LiCl (pH 7.5). Crystals appeared within a couple of days at the bottom and edges of the well of the button. The crystals of CPA·inhibitor complex were then prepared by incubating the CPA crystals in the low salt buffer containing the inhibitor (1:3 molar ratio). Because severe cracking occurred when the protein crystals were soaked in the inhibitor-containing buffer, they were kept in the cross-linking solution (0.02 M Hepes, 0.1 M LiCl at pH 7.5 containing 0.01% Dimethyl Suberimidate) for 120 min before transfering into the inhibitor-containing buffer. Although the crystals cracked even after the cross-linking, the crystals could be handled without fragmentation. The crystals in the soaking solution were stored in a cold room (277 K) for 3 days before data collection.

Data collection, structure determination, and refinement

All diffraction data were measured on a DIP2000 area detector with graphite monochromated CuK_α X-rays generated by a MacScience M18XHF rotating anode generator operated at 90 mA and 50 kV at room temperature. Data reduction, merging, and scaling were accomplished with the programs DENZO and SCALEPACK.[11] The total numbers of independent reflections with $I>2\,\sigma$ used in the structure refinement of CPA•D-**1**, CPA•L-**1** and CPA•L-**2** were 12,659 (96%), 93,237 (88.5%) and 93,239 (81.6%), respectively. The statistics of the data are shown in Table 3.

Table 2. Selected bond distances (Å) in CPA·inhibitor complexes

Atoms in interaction[a]	CPA•L-1[b]	CPA•D-1	CPA•L-2[b]
$Zn^{2+}\cdots O^3$	2.06	—[c]	2.05
$Zn^{2+}\cdots O^4$	—	2.17	N/A[d]
Glu^{270}–$O^1\varepsilon\cdots O^4$	2.91	—	N/A
Glu^{270}–$O^2_\varepsilon\cdots O^4$	2.84	2.67	N/A
Glu^{270}–$O^1_\varepsilon\cdots N^1$	2.67	—	2.66
Glu^{270}–$O^2_\varepsilon\cdots N^2$	—	—	3.18
Arg^{145}–$N^1_\eta\cdots O^1$	3.03	2.82	3.03
Arg^{145}–$N^2_\eta\cdots O^2$	2.94	3.19	2.94
Arg^{127}–$N^1_\eta\cdots O^1$	3.00	—	3.00
Arg^{127}–$N^1_\eta\cdots O^2$	—	3.14	—
Tyr^{248}–$O_\eta\cdots O^1$	—	2.94	—
W^1–$O\cdots O^1$	2.88	N/A	2.88
$W^1-O\cdots O_\eta-Tyr^{248}$	3.13	N/A	3.13
$W^2-O\cdots O^3$	N/A	2.75	N/A
$W^2-O\cdots-Tyr^{198}$	N/A	2.94	N/A

[a]Numbering of inhibitor atoms is shown in the structure of the inhibitors.
[b]Three bond distances are average values of four complexes present in an asymmetric unit.
[c]'–' denotes that hydrogen bond is not observed between the atoms.
[d]N/A denotes not applicable.

The crystals of CPA•D-**1** complex belonged to the monoclinic space group $P2_1$ with the cell dimensions of $a=51.961$ Å, $b=60.465$ Å, $c=47.792$ Å, and $\beta=97.591$. There is one molecule of the complex per asymmetric unit. The crystals of CPA•L-**1** and CPA•L-**2** belonged to the triclinic space group $P1$ with cell dimensions of $a=65.572$ Å, $b=60.524$ Å, $c=74.410$ Å, $\alpha=90.0$, $\beta=97.845$, and $\gamma=90.0$, and contain four molecules of the complex per asymmetric unit (Table 3). While D-**1**

Table 3. Summary of the crystallographic data

	CPA·L-**1**	CPA·D-**1**	CPA·L-**2**
X-ray source	Cu*K*	Cu*K*	Cu*K*
Wavelength (Å)	1.5418	1.5418	1.5418
Resolution range (Å)	20.0–1.75	20.0–2.30	20.0–1.75
R_{sym}[a]	4.8 (17.9)	6.0 (9.4)	4.6 (14.9)
Completeness			
($>1\sigma$, %)	90.3	96.0	90.4
(outer shell, Å)	77.0 (1.86–1.80)	82.2 (2.38–2.30)	77.4 (1.97–1.90)
Number of refined atoms			
protein/solvent/inhibitor	7311/591/48	2443/211/16	7311/589/45
R-factor/R_{free} ($>1\sigma$, %)[b]	19.8/22.9	13.9/17.4	18.7/21.9
r.m.s. deviation			
Bond length (Å)	0.006	0.006	0.005
Bond angle (°)	1.254	1.172	1.235
Space group	*P*1	$P2_1$	*P*1
Unit cell			
a/*b*/*c*	65.572/60.524/74.410	51.961/60.465/47.792	65.572/60.524/74.410
α/β/γ	90.0/97.845/90.0	90.0/97.591/90.0	90.0/97.845/90.0

[a] $R_{sym} = \sum|I_{obs} - I_{avg}| / \sum I_{obs}$.

[b] R-factor $= \sum||F_o|-|F_c|| / \Sigma|F_o|$, where $|F_o|$ and $|F_c|$ are the observed and the calculated structure factor amplitudes, respectively. R_{free} was calculated with 5% of the data.

did not change the space group of the native crystals upon soaking, L-**1** and L-**2** resulted in change of the space group from $P2_1$ to *P*1. However, the crystal packing of the protein molecules in the space group *P*1 is nearly identical to that in the space group $P2_1$, as indicated by the very similar cell parameters except for the area of *ac* plane (2-fold difference) between the two space groups.

The structures of CPA·inhibitor complexes were determined by the molecular replacement method using AMoRe,[12] based on the atomic coordinates (excluding the active site water molecules) of the native CPA (PDB code: 5cpa). After the initial rigid body, positional, and B-factor refinements, the strand containing Tyr-248 was rebuilt, since the electron density indicated that side chain of Tyr-248 moves to the down position upon binding of the inhibitors. At this stage, the $|F_O| - |F_C|$ difference Fourier map showed clearly an extra electron density for a bound inhibitor. Initial coordinates for each inhibitor were determined by positioning the inhibitor model which was built using the program Quanta (Molecular Simulations Inc., Version 2) into the inhibitor density in the $2|F_O| - |F_C|$ map.[13] The water molecules that are present at the active site of native CPA were incorporated manually into the difference Fourier electron density maps. Subsequent several rounds of refinements and manual rebuilding decreased the R value to below 20.0%. The structures were refined with the program CNS.[14]

Acknowledgements

This work was supported by the Korea Research Foundation through Center for Biofunctional Molecules, and National Creative Research Initiatives of the Korean Ministry of Science and Technology and National Laboratory for Protein Engineering.

References and Notes

1. Guiocho, F. A.; Lipscomb, W. N. *Adv. Protein Chem.* **1971**, *25*, 1.
2. Christianson, D. W.; Lipscomb, W. N. *Acc. Chem. Res.* **1989**, *22*, 62.
3. Phillips, M. A.; Fletterick, R.; Rutter, W. J. *J. Biol. Chem.* **1990**, *265*, 20692.
4. Ondetti, M. A.; Rubin, B.; Cushman, D. W. *Science* **1977**, *196*, 441.
5. Patchett, A. A.; Harris, E.; Tristram, E. W.; Wyvratt, M. J.; Wu, M. T.; Taub, D.; Peterson, E. R.; Ikeler, T. J.; ten Broeke, J.; Payne, L. G.; Ondeyka, D. L.; Thorsett, E. D.; Greenlee, W. J.; Lohr, N. S.; Hoffsommer, R. D.; Joshua, H.; Ruyle, W. V.; Rothrock, J. W.; Aster, S. D.; Maycock, A. L.; Robinson, F. M.; Hirschman, R.; Sweet, C. S.; Ulm, E. H.; Gross, D. M.; Vassil, T. C.; Stone, C. A. *Nature* **1980**, *288*, 280.
6. Gafford, J. T.; Skidgel, R. A.; Erdos, E. G.; Hersh, L. B. *Biochemistry* **1983**, *22*, 3265.
7. Kim, D. H.; Guinosso, C. J.; Buzby, G. C., Jr.; Herbst, D. R.; McCaully, R. J.; Wicks, T. C.; Wendt, R. C. *J. Med. Chem.* **1983**, *26*, 394.
8. Powers, J. C.; Harper, J.W. In *Proteinase Inhibitors*; Barrett, A. J., Salvesen, G. Eds. Elsevier: Amsterdam, 1986; Chapter 6
9. Chung, S. J.; Kim, D. H. *Bioorg. Med. Chem.* **2001**, *9*, 185.
10. Harmon, R. E.; Dabrowiak, J. C.; Brown, D. J.; Gupta, S. K.; Herbert, M.; Chitharanjan, D. *J. Med. Chem.* **1970**, *13*, 577.
11. Otwinowski, Z.; Minor, W. *Methods Enzymol.* **1997**, *276*, 307.
12. Navaza, J.; Saludjiam, P. *Acta Crystallogr. Sect. A* **1994**, *450*, 157.
13. Jones, T. A.; Kjeldgaard, M. *O Version 5*; 9; Uppsala University: Uppsala: Sweden, 1993.
14. Brünger, A. T.; Adams, P. D.; Clore, G. M.; Delano, W. L.; Gros, P.; Grosse-Kunstleve, R. W.; Jiang, J. S.; Kuszewski, J.; Nilges, M.; Pannu, N. S.; Read, R. J.; Rice, L. M.; Simonson, T.; Warren, G. L. *Acta Crystallogr., Sect. D* **1998**, *54*, 905.
15. Rees, D. C.; Lewis, M.; Lipscomb, W. N. *J. Mol. Biol.* **1983**, *168*, 367.
16. Christianson, D. W.; Lipscomb, W. N. *Proc. Natl. Acad. Sci. U.S.A.* **1986**, *83*, 7568.
17. Schwarzenbach, G.; Schwarzenbach, K. *Helv. Chim. Acta* **1963**, *46*, 1390.

18. Nishino, N.; Powers, J. C. *Biochemistry* **1978**, *17*, 2846.
19. Bode, W.; Reinmer, P.; Huber, R.; Kleine, T.; Schnierer, S.; Tschesche, H. *EMBO J*. **1994**, *13*, 1263.
20. Holmes, M. A.; Matthews, B. W. *Biochemistry* **1981**, *20*, 6912.
21. Bertini, L.; Luchinat, C.; Messori, L.; Monnanni, R.; Auld, D. S.; Riodan, J. E. *Biochemistry* **1988**, *27*, 8318.
22. Bicknell, R.; Schaffer, A.; Bertini, L.; Luchinet, C.; Vallee, B. L.; Auld, D. S. *Biochemistry* **1988**, *27*, 1050.
23. Christanson, D. W.; Mangani, S.; Shoham, G.; Lipscomb, W. N. *J. Biol. Chem*. **1989**, *264*, 12849.
24. Luchinat, C.; Monnanni, R.; Relens, S.; Vallee, B. L.; Auld, D. S. *J. Inorg. Biochem*. **1988**, *32*, 1.
25. Banci, L.; Schroeder, S.; Kollman, P. A. *Proteins Struct. Funct. Genet*. **1992**, *13*, 288.
26. Gillespie, L., Jr.; Oates, J. A.; Crout, J. R.; Sjoerdsma, A. *Circulation* **1962**, *25*, 281.